

ARTICLES

Femtosecond Fluorescence Anisotropy Studies of Solvation-Induced Intraligand Charge Transfer in Photoexcited Aluminum(III) Tris(8-hydroxyquinoline)

E. van Veldhoven, H. Zhang, and M. Glasbeek*

*Laboratory for Physical Chemistry, University of Amsterdam, Nieuwe Achtergracht 129, 1018 WS Amsterdam, The Netherlands**Received: September 28, 2000; In Final Form: December 11, 2000*

For the organic light emitting diode compound aluminum(III) tris(8-hydroxyquinoline) (Alq_3), dissolved in dimethylformamide (DMF), the time dependence of the fluorescence anisotropy has been studied using the femtosecond fluorescence upconversion technique. Upon excitation within the first absorption band, near 364 nm, with polarized laser pulses of duration less than 150 fs, an initial fluorescence anisotropy of about 0.2 is found to rapidly decay with a time constant of 2.0 ± 0.2 ps. The observed fast anisotropy decay component is concomitant with the solvation-induced dynamic Stokes shift of about 1000 cm^{-1} . When excitation is at wavelengths below 330 nm, the fluorescence of Alq_3 in liquid solution does not show any anisotropy effect. It is discussed that the emissive lowest excited electronic state of Alq_3 is ligand localized and that its electronic wave function is affected by solvation. More specifically, the electronic wave function is considered to be an admixture of wave functions belonging to several close-lying states. Upon pulsed optical excitation, the admixture is assumed to vary with time, the time dependence being determined by the time evolution of the generalized solvation coordinate. The solvation-induced changes of the excited-state wave function effectuates a directional change of the emission transition dipole moment and thus gives rise to a temporal dependence of the fluorescence anisotropy. The rotational motions of the Alq_3 solute molecules also contribute to the fluorescence anisotropy decay. However, these motions occur on a much slower time scale (about 100 ps). A comparative study of the fluorescence anisotropy decay of Alq_3 in different solvents shows that the rotational motions of the Alq_3 molecules follow the Debye–Stokes–Einstein relation.

1. Introduction

Aluminum (III) tris(8-hydroxyquinoline) (Alq_3) has been successfully applied as emitting material in organic light emitting diodes (OLED).^{1–5} Small-molecule-based OLEDs have great potential for use in optoelectronic devices and flat panel display technology.^{6,7} Most studies concern the morphology of Alq_3 in amorphous thin films and in different crystalline forms,^{8–10} the optimization of the devices,⁶ and the mechanisms and dynamics of charge injection, charge transport, and charge recombination.^{11,12} Relatively few studies have been devoted to the fluorescence of Alq_3 , although such studies are important for understanding the electrooptical properties on a molecular level. The fluorescence data, in solution^{2,13,14} and in thin films,^{6,10} indicate that the relevant lowest excited electronic states are localized on the individual quinolate ligand molecules. This is noteworthy because uncomplexed 8-hydroxyquinoline in many organic solvents is only weakly fluorescent, or even nonfluorescent.¹⁵ Complexation with metal ions, however, may induce a fluorescence enhancement (fluorogenic effect). Semiempirical molecular orbital^{16,17} and density functional theory (DFT) calculations^{16,18} provided insight into the electronic charge distributions of Alq_3 and metal– Alq_3 complexes¹⁹ in ground and excited states. Photoabsorption gives rise to $\pi\pi^*$ excitations

at the quinolate ligand for which the electronic charge is partially transferred from the phenoxide to the pyridyl ring (intraligand charge transfer).^{6,12,17}

Very recently, we reported the first ultrafast fluorescence upconversion studies of Alq_3 , in solution²⁰ and in vapor-deposited thin films.²¹ For Alq_3 , in solution, picosecond fluorescence transients were resolved. Analysis of the temporal spectral behavior showed that the picosecond components are due to solvation effects that occur after pulsed optical excitation. Interestingly, it was also observed that the solvation-induced dynamic Stokes shift is accompanied by a decrease of the integrated fluorescence intensity much faster than can be accounted for by the ν^3 -law for spontaneous emission. To explain this drop of the emission intensity, we conjectured that during solvation the excited-state adiabatic potential energy surface and, concomitantly, the excited-state electronic wave function are changed. Solvent-induced mixing of close-lying excited molecular states was considered to account for the change of the excited-state radiative character.²⁰

In this paper, we report a femtosecond time-resolved fluorescence anisotropy study of the relaxation processes of Alq_3 that take place after photoexcitation. Time-resolved fluorescence anisotropy spectroscopy, performed on a time scale that exceeds that of the rotational diffusion motions of the molecules in the liquid (for our molecules ~ 50 ps, or more, *vide infra*), is a powerful tool for revealing intramolecular

* Corresponding author. FAX: +31 20 5256994. E-mail: glasbeek@fys.chem.uva.nl.

dynamics.^{22–24} In the case of photoexcited Alq₃, one may expect that dynamic anisotropy fluorescence measurements provide a sensitive test for the proposed solvation-controlled charge redistribution in the molecule. It will be shown in this paper that the femtosecond fluorescence anisotropy experiments indeed give independent evidence for (i) the localized nature of the emissive state and (ii) excited-state electronic charge redistribution dynamics pertinent to the solvation process.

2. Experimental Section

Alq₃ was purchased from Aldrich and used without further purification. Dimethylformamide (DMF) and ethylene glycol are of spectrophotometric grade (Aldrich). Samples with a concentration of 10⁻⁴ M were used for the measurements.

Femtosecond and picosecond polarized fluorescence transients were measured by means of two experimental setups. Femtosecond laser excitation was accomplished using a diode-pumped CW Nd:YVO₄ laser (Spectra Physics, Millennia X) which pumped a Ti:sapphire laser (Spectra Physics, Tsunami) operating at 800 nm and which delivered 60 fs pulses at a repetition rate of 82 MHz. The laser pulses were first amplified in a regenerative amplifier laser system (Quantronix) to about 400 mW at 1 kHz, and then split into two beams. One of the beams was led into a TOPAS laser system (Light Conversion Ltd.) that produced the excitation pulses. To avoid heating of the sample, the latter was motor-driven back and forth perpendicular to the direction of the TOPAS laser beam. The photoinduced transient fluorescence was time-resolved by applying the fluorescence upconversion detection technique.^{25,26} The second part of the fundamental beam (800 nm) was led through an optical delay line and focused together with the induced fluorescence onto a 1 mm thick BBO crystal (type I phase matching condition). The upconversion signal (at the sum frequency of the fluorescence and the fundamental of the femtosecond laser) was filtered out by a UG 11 filter, and then focused on the entrance slit of a monochromator and photodetected using a photomultiplier connected to a lock-in amplifier. By means of a polarizer in front of the sample, the polarization of the excitation beam was chosen parallel or perpendicular to the polarized gating beam. From the measured cross-correlation function of the excitation and gating pulses at 400 and 800 nm, the instrumental time response was estimated to be approximately 150 fs (fwhm).

Fluorescence transient measurements with picosecond time resolution were conducted using the time-correlated single-photon-counting (TCSPC) technique.²⁷ Briefly, a mode-locked Ar⁺ ion laser (Coherent, Innova 200-15) synchronously pumped a dye laser (Coherent, 702-3) with a cavity dumper (Coherent, 7200). The cavity-dumped dye laser generated laser pulses of about 7 ps (fwhm autocorrelation trace), with an energy of about 25 nJ at 3.7 MHz. These pulses were frequency doubled in a 6 mm BBO crystal and used to photoexcite the sample. The fluorescence transients were detected applying the time-correlated single-photon-counting technique in reverse mode. The instrument response was about 16 ps (fwhm). All fluorescence transients were measured at parallel and perpendicular polarization directions with respect to the polarization of the excitation light.

Steady-state absorption spectra were recorded by means of a conventional spectrophotometer (Shimadzu, UV-240). Steady-state fluorescence spectra were measured using the emission spectrometer described before.²⁷ The emission spectra were

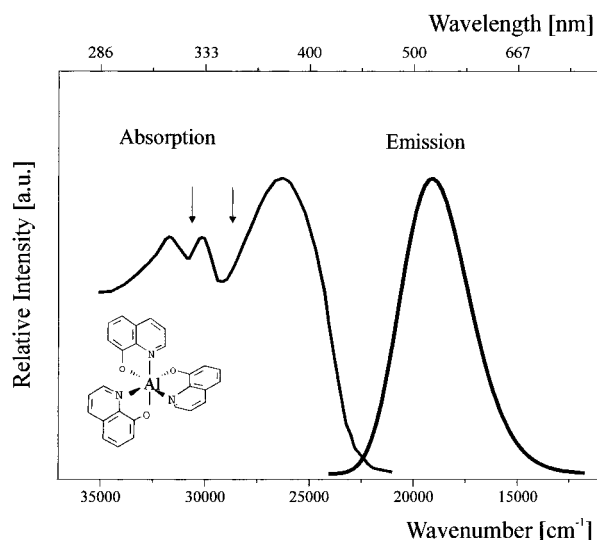


Figure 1. Absorption and emission spectra of Alq₃ dissolved in DMF. Arrows indicate positions of the excitation wavelengths (326 and 360 nm) used in the fluorescence transient measurements.

corrected for the wavelength-dependent sensitivity of the monochromator–photomultiplier detection system.

3. Results

In Figure 1 we have reproduced the steady-state absorption and emission spectra for Alq₃ in DMF given previously.²⁰ The first absorption band peaks at 26 800 cm⁻¹; two less intense peaks are found at 30 000 and 32 000 cm⁻¹. The spectrum is similar to that reported recently for Alq₃ in CH₂Cl₂.²⁸ The emission spectrum is independent of the excitation wavelength within the absorption range and in good agreement with the photoluminescence spectrum reported elsewhere.²⁹

Recently, we reported femtosecond fluorescence upconversion transients for Alq₃ dissolved in DMF, dimethyl sulfoxide (DMSO), dichloromethane, and toluene.²⁰ Measurement of the fluorescence upconversion transients under magic angle conditions yields, in the blue part of the emission band (460 nm < λ < 600 nm), a decay; the transients detected in the red part of the emission (600 nm < λ < 645 nm) display a rise. After spectral reconstruction, the dynamic Stokes shift to the red for Alq₃ in DMF was determined to be about 1000 cm⁻¹. The time dependence of the spectral shift, at room temperature, is exponential with a time constant of 1.9 ± 0.2 ps. This value is also the value of the solvent relaxation time for DMF.³⁰ It was thus found that the dynamic Stokes shift that follows the pulsed excitation can be attributed to the solvation process. Here we consider the anisotropy dynamics of the fluorescence that can be measured while solvation takes place for Alq₃ in DMF.

Using linearly polarized excitation pulses, transients have been measured for the emission polarized parallel (*I*_{||}) and perpendicular (*I*_⊥) to the polarization direction of the exciting laser pulses. A few typical polarized upconversion transients, in a time window of 10 ps, excitation wavelength at 364 nm, are displayed in Figure 2. (The positions of the excitation wavelengths at 364 and 326 nm for the transients presented in this work are indicated by the arrows in Figure 1.) The short-time components in the fluorescence anisotropy (Figure 2a) could be resolved only when excitation is at a wavelength longer than about 340 nm (i.e., within the lowest absorption band, Figure 1). Fluorescence transients obtained for 326 nm and shorter excitation wavelengths did not exhibit a temporal difference for *I*_{||}(*t*) and *I*_⊥(*t*).

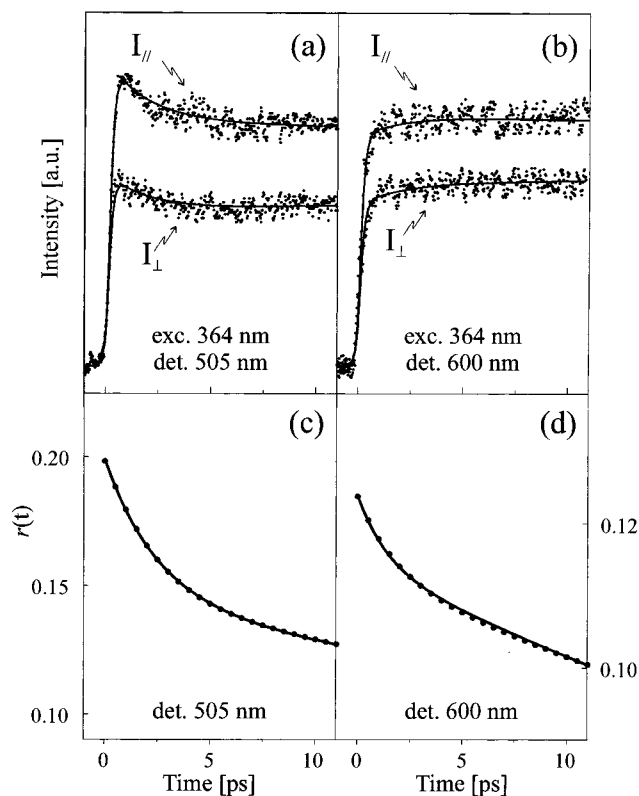


Figure 2. Polarized fluorescence upconversion transients of Alq₃ in DMF as detected at 505 (a) and 600 nm (b); excitation wavelength is 364 nm. Solid lines are best fits to biexponential function convoluted with system response function. The time dependence of the fluorescence anisotropy, $r(t)$, as obtained from the best-fit functions in (a) and (b) are given in (c) and (d), respectively.

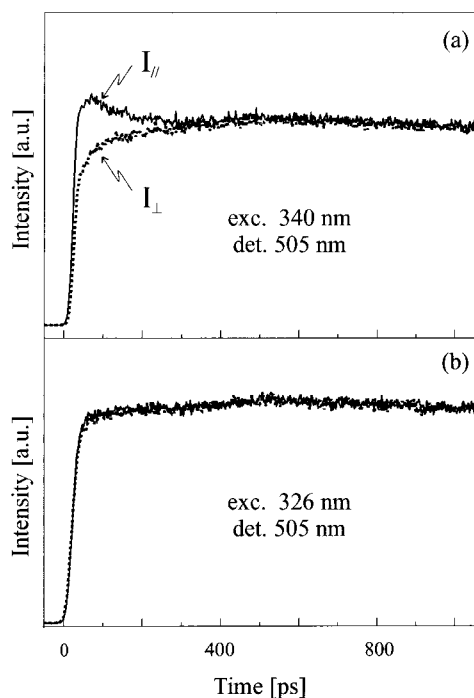


Figure 3. Polarized fluorescence transients for Alq₃ in DMF as measured with TCSPC setup with excitation at 340 (a) and 326 nm (b); detection is at 505 nm. In (b), the parallel and perpendicular polarized transients coincide.

The time span was expanded in the TCSPC measurements. As illustrated in Figure 3a, for the transients obtained with the excitation at 340 nm, anisotropy persists up to about 300 ps.

TABLE 1: Fluorescence Anisotropy Decay Times Characteristic of the Best-Fit Biexponential Function for $r(t)$ for Alq₃ Dissolved in DMF^a

detection wavelength (nm)	τ_1 (ps)	τ_2 (ps)	τ_{solv} (ps)
505	2.5 ± 0.2 (0.06)	85 ± 5 (0.14)	1.9
600	1.4 ± 0.2 (0.01)	85 ± 5 (0.11)	

^a The relative weights of the components are given in parentheses. The solvent relaxation time, τ_{solv} , is from ref 30.

As before, when excitation is at 326 nm, $I_{||}(t)$ and $I_{\perp}(t)$ behave alike with no difference between them.

The femtosecond upconversion and the picosecond TCSPC transients were each fitted with a biexponential function convoluted with the system response function. The tails of the fitted decay curves for the upconversion transients matched the fitted curves of the transients obtained with the time-correlated single-photon-counting setup. The drawn curves in Figure 2a,b show the best-fit convoluted biexponential curves.

The time-resolved anisotropy, defined as

$$r(t) = \frac{I_{||} - I_{\perp}}{I_{||} + 2I_{\perp}} \quad (1)$$

was obtained from the best fit functions for $I_{||}(t)$ and $I_{\perp}(t)$. Note that in eq 1 and hereafter $I_{||}(t)$ and $I_{\perp}(t)$ refer to fluorescence intensities obtained after deconvolution of the experimental fluorescence transients. The best-fit functions for $r(t)$ characteristic of the transients obtained with the excitation at 364 nm and detection at 505 and 600 nm are given as drawn curves in parts c and d, respectively, of Figure 2. Likewise, the temporal behavior of the fluorescence anisotropy for the TCSPC transients was determined. The best-fit values for the “fast” and “slow” anisotropy time constants and the relative weights of the corresponding components have been collected in Table 1. For comparison the table includes the characteristic solvation times for Alq₃ in DMF as determined from the dynamic Stokes shift measurements.²⁰

4. Discussion

Alq₃ is an organometal trischelate with a distorted octahedral coordination. The two geometrical isomers of Alq₃, the “meridional” (mer) isomer and the “facial” (fac) isomer, are chiral and thus correspond to two different optical isomers.⁶ DFT-based calculations predict that the mer isomer is lower in energy but fac has a higher dipole moment. It is reasonable to expect that in the liquid phase both isomers coexist.^{10,18} As has been discussed recently on the basis of DFT and semiempirical calculations, photoabsorption leads to a ligand-localized excitation.^{17,18} For the case that the transition moments of the absorption and emission dipoles are parallel, the theoretical value for the initial fluorescence anisotropy becomes $r(0) = 0.4$.^{31,32} The plots in Figure 2c,d illustrate that $r(0)$ is nonzero. The nonzero anisotropy signifies that, within the system response time of 150 fs, the directions of the transition moments of the absorption and emission processes remain, at least partially, correlated. The values of 0.2 (detection at 505 nm) and 0.12 (detection at 600 nm), are lower than the theoretical limit of 0.4. This lowering is likely due to a diminished photoselectivity by the polarized excitation because of spectral overlap of several absorption bands (with different polarization) at the experimental excitation wavelengths (340–360 nm). Such a spectral overlap effects that the emissive state is populated by relaxation from different electronic excited states. Consequently, the directional

correlation between the absorption and emission dipoles is partially lost and values for $r(0)$ lower than 0.4 will be obtained. Note that in this view the emissive state in part has attained its initial population after internal conversion from one or more other higher-lying electronically excited states. It follows that the internal conversion process must be ultrafast and completed within the system response time of 150 fs. Such an ultrafast interligand relaxation phenomenon was reported previously also for another metal complex, namely $\text{Ru}(\text{bpy})_3^{2+}$.³³ Moreover, when excitation is at 326 nm or shorter wavelengths, no rise component can be observed for the femtosecond fluorescence upconversion transients. This result further supports that internal conversion is within the 150 fs system response time.

An alternative possibility for the lowering of the maximal value of the anisotropy is that, within the first 150 fs after the excitation pulse, the emissive state is already populated but during that time span solvation dynamics affects the electronic wave function. This is the process considered previously to explain the variation of the total fluorescence intensity that accompanies the dynamic Stokes shift.²⁰ Calculations have indicated that Alq_3 has a number of close-lying excited ligand-localized electronic states near 2.8 eV.^{17,18} We argue that the solvent environment causes a mixing of these states, the mixing being dependent on the degree of the solvation process, i.e., the value of the generalized solvation coordinate. If it is assumed that the solvation-controlled changes of the electronic wave function result also in a change in the direction of the fluorescence transition moment, then this will lower the value of $r(0)$. (Tilting the angle between the absorption and emission dipoles by 35° leads to an anisotropy of 0.2.) Very fast solvation dynamics, on a time scale of 100 fs or less, is well-known and is commonly attributed to inertial reorientational motions of the solvent molecules.^{34,35} Thus the lowering of the fluorescence anisotropy value from 0.4 to 0.2 (within 150 fs) could also be due to the effects of inertial free streaming solvent motions on the nature of the electronic wave function of Alq_3 in the fluorescent state. It should be added that a change in the anisotropy due to solvent-induced mixing of different electronic levels is only possible when the mixing involves several *radiative* electronic levels. Mixing in the region of conical intersection of the fluorescent and the electronic ground states, for instance, may be ruled out, because such a mixing would not affect r . Very recently, we have verified this feature for auramine.³⁶ For the latter, it was established by means of time-resolved transient absorption and emission experiments that the excited-state dynamics is determined by a solvent-controlled admixture of emissive and *nonemissive* excited states.^{37,38} Mixing these states thus can affect the fluorescence quantum yield but cannot change the direction of the emissive dipoles, and no temporal dependence of r is expected. This is exactly what has been found experimentally.³⁶

As noted above, $r(0)$ values of 0.2 and 0.12 are obtained when detection is at 505 and 600 nm, respectively. Since the emissions detected at 505 and 600 nm have in the optical transition the final electronic state in common (namely, the electronic ground state), the different initial anisotropy values can only arise because the initial states are of different radiative character. This difference is readily argued on the basis of the above-mentioned ultrafast solvation mechanism. The “600 nm” emission is due to molecules that have progressed further in the solvation process than the molecules emitting at “505 nm”. In the meantime the fluorescence anisotropy may have changed. The different values for $r(0)$ obtained at 505 and 600 nm are therefore a further

indication of an ultrafast solvation-induced initial electronic relaxation. In summary, we considered two possible mechanisms for the lowered values of $r(0)$, i.e., overlapping excitations and solvation dynamics leading to ultrafast electronic relaxation. Most probably, both mechanisms apply in the case of Alq_3 in DMF.

Anisotropy effects in the fluorescence are not observed when excitation is at photon energies higher than about $30\,000\text{ cm}^{-1}$. Calculations show that at these energies several, almost isoenergetic, electronic states with different directions for their transition moments may be excited.^{17,18} Therefore, excitation near 3.7 eV or higher energies most likely causes branching; i.e., several electronic states with different directions for their transition moments are simultaneously excited. Under such conditions, photoselection by the polarized laser pulses does not occur, thus excluding polarized emission.

The biexponential decay of the fluorescence anisotropy of Alq_3 in DMF (Figure 2c,d), with time constants of 2.0 and 85 ps, reveals that, apart from the ultrafast (<150 fs) initial dynamics, several relaxation processes affect Alq_3 in the excited state. The fluorescence depolarization data at early times (up to about 10 ps) show that in this time regime the dynamics of the depolarization process compares very well with that of the dynamic Stokes shift (with a time constant of about 2.0 ps (ref 20)) and the solvent relaxation time of 1.7 ps of the solvent.²⁶ Moreover, for Alq_3 doped in an $\text{Al}(\text{acac})_3$ host crystal, no picosecond Stokes shift or fluorescence depolarization transients were observed. Similarly, in a methanol and ethanol (1:3) solution at room temperature only a 80 ps fluorescence anisotropy decay component is obtained, whereas a decay is absent when the alcohol mixture is cooled below the glass transition point. These findings indicate that the 2.0 ps fluorescence anisotropy decay must be attributed to solvation. The time scale corresponds to that typical of rotational diffusion motions of the solvent molecules.³⁹

A major finding in this study is that solvation can affect the temporal behavior of the fluorescence anisotropy. Normally, solvation takes place with the system in a single excited electronic state with a well-defined transition dipole moment for the emission to the ground state. In other words, solvation is usually not accompanied by a change of the electronic wave function of the excited state and a temporal change in the direction of the electronic transition dipole is not expected. However, in the model discussed above for photoexcited Alq_3 in solution, a solvation-induced mixing of nearby excited electronic states of different radiative character is adopted. Different directions for the optical dipole transition moments of the admixed states will then lead to a temporal change of r as solvation progresses. The equal time constants for the anisotropy decay and the solvation dynamics are in favor of this model. We conclude that the time-resolved anisotropy measurements for Alq_3 in solution provide further support for the idea that the emissive excited state is affected by the solvation process.

It might be considered that the excited electronic states of Alq_3 that become dynamically mixed in the solvation process concern delocalized states that may originate from equivalent excited states of the three ligands. In this picture, the solvation process assists in the formation of a localized excitation at one of the ligand molecules. However, in the case of femtosecond laser pulse excitation of almost degenerate electronic states, initially high values (>0.5) for the fluorescence anisotropy may be expected.⁴⁰ The fluorescence anisotropy results obtained for Alq_3 show values much lower than 0.4, however. This indicates

TABLE 2: Characteristic Time, τ_2 , for the “Long” Fluorescence Anisotropy Decay Component for Alq₃, Gaq₃, and Inq₃, Dissolved in DMF and Ethylene Glycol^a

metal complex	DMF			ethylene glycol		
	τ_2 (ps)	τ_r (ps)	R (Å)	τ_2 (ns)	τ_r (ns)	R (Å)
Alq ₃	85	85	4.7	1.18	1.18	4.15
Gaq ₃	91	91	4.8	1.28	1.27	4.25
Inq ₃	122	105	5.0			

^a The rotational diffusion times estimated from the Debye–Stokes–Einstein (DSE) relation as indicated in the text are included.

that, at least after 150 fs, electronic dephasing has already occurred⁴⁰ and that the fluorescence is most likely due to a ligand-localized state. Moreover, as already remarked above, calculations indicate close-lying excited *ligand-localized* electronic states near 2.8 eV.^{17,18} The redirection of the transition dipole moment that can be associated with the temporal fluorescence anisotropy is most likely related to the intraligand charge separation that has been proposed to characterize the ligand-localized photoexcitation of Alq₃.¹⁸

After optical excitation near 360 nm, the Alq₃ molecules are also vibrationally excited. In discussing the fluorescence transients of Figure 2, we should thus also consider the possibility of hot band emission. In the latter event, the 2.0 ps fluorescence decay component could refer to the vibrational relaxation time of the vibrationally hot Alq₃ molecules,⁴¹ and thus need not arise from solvation dynamics. To investigate this possibility, time-resolved fluorescence anisotropy measurements were performed for Alq₃ dissolved in a methanol–ethanol 1:3 glass. The result is, as mentioned above, a total lack of dynamic anisotropy effects in the fluorescence. Moreover, when the measurements of the anisotropy time dependence were repeated in the solvents DMSO and CH₂Cl₂, the picosecond decay component of $r(t)$ was found to vary in accordance with the respective solvent relaxation times. It is concluded that the fluorescence anisotropy decay dynamics is not determined by vibrational relaxation (hot emission decay).

Strictly speaking, if for a sharply defined detection wavelength only the response of the system for a well-defined value of the generalized solvation coordinate would be probed, then the system has a well-defined anisotropy value that would not be time dependent. It is therefore necessary to examine how it is possible that, when the measured fluorescence at a particular wavelength, say 505 nm, is due to a single electronic state (without any hot band emission), the fluorescence anisotropy can still show a 2.0 ps time component. The first contribution to consider is inhomogeneous broadening (IB). IB arises from the spread in the solvation coordinate, thus leading to a population distribution in the excited state related to the spread in the solvation coordinate.²⁶ Emission is therefore not due to states corresponding to a fixed value of the solvation coordinate only, but the spread in the latter at a fixed wavelength causes the response from a population distribution giving rise to a spread in the emission anisotropy to be detected. Since this distribution develops in time, a time-dependent anisotropy is observed. Moreover, in our experiments the detection wavelength is not infinitely sharp, but has a spread of about 5 nm. Thus the limited spectral resolution of approximately 5 nm also contributes to the temporal behavior of $r(t)$.

Finally, we briefly discuss the slow decay component in the fluorescence anisotropy decay (Table 1). Again, we find that the fluorescence anisotropy is observed only when the excitation wavelength is above 344 nm; i.e., the photon excitation energy is kept as low as possible. The decay with time of $r(t)$, as extracted from the convoluted TCSPC transients for $I_{\parallel}(t)$ and

$I_{\perp}(t)$, is found to be monoexponential. The best-fit function has a characteristic decay time of 85 ps for Alq₃ in DMF. The decay time becomes much longer in high-viscosity solvents. For instance, in ethylene glycol the decay time is 1.18 ns (Table 2). The “long” (85 ps) fluorescence anisotropy decay component is present only when the complexes are in liquid solution. Also, $r(t)$ appears to be independent of the detection wavelength. These features are typical of fluorescence anisotropy decay arising from rotational diffusion motions of the probed solute molecules. Such motions are usually considered in fluorescence anisotropy studies.³¹

Table 2 comprises the results for the experimental fluorescence anisotropy decay times, τ_2 , for a number of Mq₃ complexes, with M = Al, Ga, or In. It appears that these anisotropy decay times are compatible with the rotational diffusion times obtained from the Debye–Stokes–Einstein relation⁴²

$$\gamma(t) = Ae^{-6D_S t} \quad (2)$$

where the rotational diffusion rate constant, D_S , is given as

$$D_S = \frac{k_B T}{8\pi\eta R^3} \quad (3)$$

k_B is the Boltzmann constant, T is the temperature, η is the viscosity coefficient of the solvent (0.8 mPa·s for DMF, 16.1 mPa·s for ethylene glycol),⁴³ and R is the radius of the solute molecule, which in the model is assumed to have a spherical shape. In Table 2 we have included the values of the rotational diffusion times, $\tau_r = (6D_S)^{-1}$, as obtained for the given R values for the Mq₃ complexes. These values for R were assumed to follow the increase of the atomic radii of Al³⁺, Ga³⁺, and In³⁺. The satisfactory agreement between the values of τ_2 and τ_r confirms that the “long” time decay component of the fluorescence anisotropy of Alq₃ in DMF is due to the rotational diffusion motions of the solute molecules indeed.

In conclusion, femtosecond fluorescence anisotropy measurements for Alq₃ in liquid solution revealed a biexponential decay behavior characterized by a “fast” (2 ps) and a “slow” (85 ps) decay component. The presence of close-lying excited states enhances the polarizability of the excited state. It has been discussed that the “fast” decay is due to the influence of solvation on the highly polarizable fluorescent excited state of Alq₃. The “slow” decay arises from the conventional influence of the rotational diffusion motions of the solute molecules.

References and Notes

- (1) Tang, C. W.; Van Slyke, S. A. *Appl. Phys. Lett.* **1987**, *51*, 913.
- (2) Tang, C. W.; Van Slyke, S. A.; Chen, C. H. *J. Appl. Phys.* **1989**, *65*, 3610.
- (3) Kido, J.; Kimura, M.; Nagai, K. *Science* **1995**, *267*, 1332.
- (4) Sheats, J. R.; Antoniadis, H.; Hueschen, M.; Leonard, W.; Miller, J.; Moon, R.; Roitman, D.; Stocking, A. *Science* **1996**, *273*, 884.
- (5) Friend, R. H.; Gymer, R. W.; Holmes, A. B.; Burroughes, J. H.; Marks, R. N.; Taliani, C.; Dos Santos, D. A.; Brédas, J.-L.; Lögdlund, M.; Salaneck, W. R. *Nature (London)* **1999**, *397*, 121.
- (6) Burrows, P. E.; Shen, Z.; Bulovic, V.; McCarty, D. M.; Forrest, S. R.; Cronin, J. A.; Thompson, M. E. *J. Appl. Phys.* **1996**, *79*, 7991.
- (7) Shen, Z.; Burrows, P. E.; Bulovic, V.; Forrest, S. R.; Thompson, M. E. *Science* **1997**, *276*, 2009.
- (8) Do, L. M.; Han, E. M.; Yamamoto, N.; Fujihira, M. *Thin Solid Films* **1996**, *273*, 202.
- (9) Alvarado, S. F.; Libiouille, L.; Seidler, P. F. *Synth. Met.* **1997**, *91*, 69.
- (10) Brinkmann, M.; Gadret, G.; Muccini, M.; Taliani, C.; Masciocchi, N.; Sironi, A. *J. Am. Chem. Soc.* **2000**, *122*, 5147.
- (11) Priestley, R.; Sokolik, I.; Walser, A. D.; Tang, C. W.; Dorsinville, R. *Synth. Met.* **1997**, *84*, 915.

- (12) Stampor, W.; Kalinowski, J.; Marconi, G.; Di Marco, P.; Fattori, V.; Giro, G. *Chem. Phys. Lett.* **1998**, *283*, 373.
- (13) Ballardini, R.; Varani, G.; Indelli, M. T.; Scandola, F. *Inorg. Chem.* **1986**, *25*, 3858.
- (14) Lytle, F. E.; Storey, D. R.; Juricich, M. E. *Spectrochim. Acta* **1973**, *29A*, 1357.
- (15) Bardez, E.; Devol, I.; Larrey, B.; Valeur, B. *J. Phys. Chem. B* **1997**, *101*, 7786.
- (16) Sugiyama, K.; Yoshimura, D.; Miyazaki, T.; Ishii, H.; Ouchi, Y.; Seki, K. *J. Appl. Phys.* **1998**, *83*, 4928.
- (17) Zhang, R. Q.; Lee, C. S.; Lee, S. T. *Chem. Phys. Lett.* **2000**, *326*, 413.
- (18) Curioni, A.; Boero, M.; Andreoni, W. *Chem. Phys. Lett.* **1998**, *294*, 263.
- (19) Curioni, A.; Andreoni, W. *J. Am. Chem. Soc.* **1999**, *121*, 8216.
- (20) Humbs, W.; van Veldhoven, E.; Zhang, H.; Glasbeek, M. *Chem. Phys. Lett.* **1999**, *304*, 10.
- (21) Humbs, W.; Zhang, H.; Glasbeek, M. *Chem. Phys.* **2000**, *254*, 319.
- (22) van Veldhoven, E.; Zhang, H.; Glasbeek, M. In *Technical Digest on Ultrafast Phenomena 2000*; Optical Society of America: Washington, DC, 2000; p 410.
- (23) Yeh, A. T.; McCusker, J. K.; Shank, C. V. In *Technical Digest on Ultrafast Phenomena 2000*; Optical Society of America: Washington, DC, 2000; p 76.
- (24) Sarkar, N.; Takeuchi, S.; Tahara, T. *J. Phys. Chem. A* **1999**, *103*, 4808.
- (25) Kahlow, M. A.; Jarzeba, W.; Dubrull, T. P.; Barbara, P. F. *Rev. Sci. Instrum.* **1988**, *59*, 1098.
- (26) Zhang, H.; Jonkman, A. M.; van der Meulen, P.; Glasbeek, M. *Chem. Phys. Lett.* **1994**, *224*, 551.
- (27) Middelhoek, E. R.; van der Meulen, P.; Verhoeven, J. W.; Glasbeek, M. *Chem. Phys.* **1995**, *198*, 573.
- (28) Brinkmann, M.; Gadret, G.; Muccini, M.; Taliani, C.; Masciocchi, N.; Sironi, A. *J. Am. Chem. Soc.* **2000**, *122*, 5147.
- (29) Burrows, P. E.; Sapochak, L. S.; McCarty, D. M.; Forrest, S. R.; Thompson, M. E. *Appl. Phys. Lett.* **1994**, *64*, 2718.
- (30) Reynolds, L.; Gardecki, J. A.; Frankland, S. J. V.; Horng, M. L.; Maroncelli, M. *J. Phys. Chem.* **1996**, *100*, 10337.
- (31) Lakowicz, J. R. *Principles of fluorescence spectroscopy*, 2nd ed.; Plenum: New York, 1999.
- (32) The molecular symmetry of the fac isomer is higher than for the mer isomer. In principle, for the fac isomer in the excited state a delocalized ligand excitation is possible and *r*-values as high as 0.7 may be obtained.
- (33) Damrauer, N. H.; Cerullo, G.; Yeh, A.; Boussie, T. R.; Shank, C. V.; McCusker, J. K. *Science* **1997**, *275*, 54.
- (34) Joo, T.; Jia, Y.; Yu, J.-Y.; Lang, M. J.; Fleming, G. R. *J. Chem. Phys.* **1996**, *104*, 6089.
- (35) De Boeij, W. P.; Pshenichnikov, M. S.; Wiersma, D. A. *Annu. Rev. Phys. Chem.* **1998**, *49*, 99.
- (36) van Veldhoven, E.; Zhang, H.; Glasbeek, M. To be published.
- (37) Changenet, P.; Zhang, H.; van der Meer, M. J.; Glasbeek, M.; Plaza, P.; Martin, M. M. *J. Phys. Chem.* **1998**, *102*, 6716.
- (38) van der Meer, M. J.; Zhang, H.; Glasbeek, M. *J. Chem. Phys.* **2000**, *112*, 2878.
- (39) Maroncelli, M. *J. Mol. Liq.* **1993**, *57*, 1.
- (40) Wynne, K.; Hochstrasser, R. M. *J. Raman Spectrosc.* **1995**, *26*, 561.
- (41) Owrutsky, J. C.; Raftery, D.; Hochstrasser, R. M. *Annu. Rev. Phys. Chem.* **1994**, *45*, 519.
- (42) Moog, R. S.; Bankert, D. L.; Maroncelli, M. *J. Phys. Chem.* **1993**, *97*, 1496.
- (43) *CRC Handbook of Chemistry and Physics*, 78th ed.; Lide, D. R., Ed.; CRC Press: New York, 1997.